

Magnetic birefringence of light in antiferromagnetic transition-metal fluorides

A. S. Borovik-Romanov, N. M. Kreines, A. A. Pankov, and M. A. Talalaev

Institute of Physics Problem, USSR Academy of Science

(Submitted December 21, 1972)

Zh. Eksp. Teor. Fiz. **64**, 1762-1775 (May 1973)

We investigated the temperature dependence of the birefringence of light in tetragonal fluorides of Mn^{2+} , Co^{2+} , and Ni^{2+} . We observed that an additional magnetic birefringence Δn_M , amounting to $\sim 5\%$ of the natural birefringence, is produced in uniaxial antiferromagnets. This effect does not depend in the main on the direction of the antiferromagnetism vector l relative to the crystallographic axes. Application of ~ 50 kOe does not affect the birefringence in MnF_2 and NiF_2 . A noticeable change occurs in the birefringence of CoF_2 in a field perpendicular to the z axis, and the crystal becomes optically biaxial. It was also observed that the magnetic birefringence Δn_M does not vanish at the antiferromagnetic transition point T_N and is observed to temperatures $\sim (2-3)T_N$, thus reflecting the temperature dependence of the short-range magnetic order. Phenomenological expressions are obtained for the tensor ϵ_{ij} of the considered crystals.

1. INTRODUCTION

A number of authors^[1,2] have shown recently that in iron garnets the effect quadratic in the magnetization (magnetic birefringence of light) is comparable in magnitude with the linear effect (the Faraday effect). Detailed experimental and theoretical investigations of the angular and temperature dependences of the magnetic birefringence in a large group of iron garnets having cubic symmetry were carried out by Pisarev, Siniĭ, Smolenskiĭ, et al.^[3,4] and by Dillon^[5]. Strong magnetic birefringence was observed also in antiferromagnets with weak ferromagnetism ($RbFeF_3$ ^[6], $\alpha - Fe_2O_3$ ^[2]).

The large values of the magnetic birefringence of light and the ease with which it can be observed have stimulated studies of this effect. Its investigation in magnetically ordered crystals has made it possible to establish the connection between the optical and magnetic characteristics of the material. This connection can be used to study, by optical means, details of the magnetic structure of crystals, the temperature dependences of the sublattice magnetizations, magnetic phase transitions, etc.

In ordinary antiferromagnets, if there is no external magnetic field there is no macroscopic magnetization. However, as shown in our preliminary communication^[7] and in the paper by Jahn and Dachs^[8], a strong change of the birefringence takes place in fluorides of transition metals when antiferromagnetic ordering occurs. The magnetic structure of the antiferromagnetic fluorides MnF_2 and CoF_2 differs from the NiF_2 structure. In addition, the external magnetic field strongly influences the magnetic structure of these crystals. To ascertain the dependence of the magnetic birefringence on the magnetic symmetry of the crystal, we have undertaken a detailed study of this effect in MnF_2 , CoF_2 , and NiF_2 in a wide range of temperatures (2 - 300°K) and magnetic fields (0 - 50 kOe).

2. SAMPLES AND NOTES ON THE METHOD

The crystals MnF_2 , CoF_2 , and NiF_2 are tetragonal; their symmetry is described by the space group D_{4h}^{14} . It is known^[9] that at low temperatures MnF_2 and CoF_2 go over into the antiferromagnetic state, and that the antiferromagnetism vector l is directed along the four-

fold axis [001]. Below T_N , NiF_2 goes over into a state with weak ferromagnetic moment m lying in a plane perpendicular to the fourfold axis and directed along the [100] or [010] axis. The vector l lies in the same plane and is perpendicular to m ^[10].

In the paramagnetic state, all these crystals are optically uniaxial. Some magnetic and optical characteristics of the investigated compounds are listed in the table. The values of T_N in the table were taken from data on the temperature dependence of the specific heat^[11], and the values of n_o and n_e are given for $T = 300^\circ K$.

The changes of the birefringence of light in the crystal were measured with the setup shown schematically in Fig. 1, by a method in which the path difference produced in the sample was directly cancelled out. The

Compound	T_N , °K	H_E , kOe	H_D , kOe	$\chi \perp \cdot 10^4$, cgs emu/mole	n_o	n_e
MnF_2	66.5	500	—	24.5	1.472	1.499
CoF_2	37.7	770	241	55	1.514	1.544
NiF_2	73.2	1130	28	6	1.525	1.560

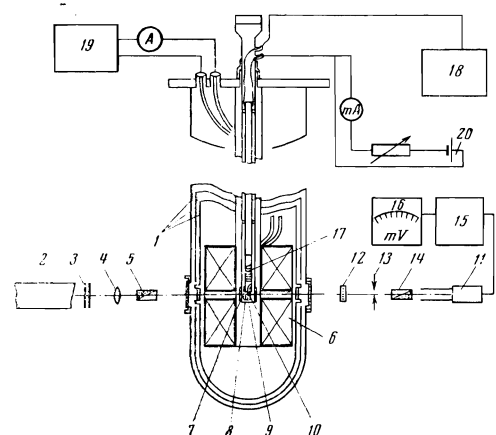


FIG. 1. Diagram of the setup for the investigation of the variation of the birefringence of light: 1—optical cryostat; 2—He-Ne laser; 3—filters; 4—lens; 5—polarizer; 6—superconducting solenoid; 7—diaphragm; 8—cell; 9—sample; 10—thermocouple junction; 11—FEU-79 photomultiplier; 12—compensator; 13—diaphragm; 14—analyzer; 15—F-116 amplifier; 16—voltmeter; 17—heater; 18—R-330 potentiometer; 19—solenoid supply; 20—heater supply.

light source (2) was an LG-126 He - Ne laser with $\lambda = 6328 \text{ \AA}$.¹¹ The sample (9), mounted inside the optical cryostat (1), was placed between two crossed polarization prisms (5 and 14). The resultant path difference Γ was compensated with a Berek calcite compensator (12)^[15]. Satisfaction of the total-compensation condition, i.e., $\Gamma_{\text{sample}} - \Gamma_{\text{comp}} = h\lambda$, where h is an integer, corresponded to a minimum of light incident on the photomultiplier (11). The measured difference between the refractive indices was $n_o - n_e = \Gamma/d$, where d is the sample thickness.

The compensator employed could measure a minimum path difference $\Delta\Gamma \sim 6 \times 10^{-3} \mu$, corresponding to a refractive-index measurement accuracy $n_o = n_e \sim 1.5 \times 10^{-6}$ at a sample thickness $\sim 4 \text{ mm}$. Actually, however, the measurement accuracy depends strongly on the quality of the investigated crystal, on its size, and also on the accuracy with which the position of the sample was duplicated in various experiments. As a result, the absolute accuracy with which $n_o - n_e$ was measured in our experiments varied from sample to sample in the range $5 \times 10^{-6} - 2 \times 10^{-5}$.

To carry out the investigations in a wide range of temperatures from 2 to 300°K, we used an optical helium cryostat (1) (Fig. 1) with a vacuum cell (8). The holder with the sample (9) was placed inside the cell on a thin-walled tube of stainless steel. The sample temperature could be varied with the aid of a heater (17) and was measured with a ZLZh-99-chromel thermocouple (10). The relative temperature-measurement accuracy was $\sim \pm 0.05^\circ$ and the absolute accuracy was $\sim \pm 0.3^\circ$ in the entire investigated interval. The magnetic field in the instrument (0 - 50 kOe) was produced with a superconducting solenoid (6).

The MnF_2 , CoF_2 , and NiF_2 single crystals were grown by S. V. Petrov²⁾ by crystallization from the melt^[16], and the optically-homogeneous crystals were selected. The samples were oriented by x-rays and were cut in the form of rectangular parallelepipeds with edges parallel to the crystallographic axes. The sample surfaces were optically polished.

3. EXPERIMENTAL RESULTS AT $H = 0$

The birefringence in the fluorides was measured in two experimental configurations: 1) the light was directed perpendicular to the optical axis [001] of the crystal,

$$k \parallel [010], \quad E \parallel [101]$$

(E is the electric vector of the light wave); 2) the light was directed along the optical axis,

$$k \parallel [001], \quad E \parallel [110].$$

The principal experimental results obtained with the first experimental configuration for MnF_2 , CoF_2 , and NiF_2 are shown in Fig. 2 in the form of temperature curves of the difference $n_o - n_e$ of the refractive indices for the ordinary and extraordinary rays. It should be noted that for the investigated crystals, the variation of $n_o - n_e$ with temperature amounted to 1-5% of the natural birefringence. Since we were interested only in the temperature dependence of $n_o - n_e$, all three curves of Fig. 2 were made to pass through zero at 300°K for convenience. We shall henceforth use the notation

$$\Delta n(T) = (n_o - n_e)_T - (n_o - n_e)_{300^\circ\text{K}}.$$

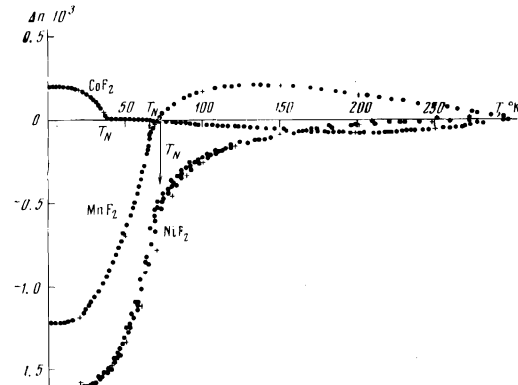


FIG. 2. Temperature dependence of the birefringence of light in MnF_2 , CoF_2 , and NiF_2 in the case when $k \parallel [010]$ and $E \parallel [101]$ ● - present data; + - data from [8, 17].

A comparison of our experimental data with those of Jahn and Dachs^[8, 17] shows good agreement of the results for MnF_2 and CoF_2 (see Fig. 2). For NiF_2 , the agreement of $\Delta n(T)$ is much worse. However, the NiF_2 sample used by us was small in size and of low grade, and the experimental data for the sample are less reliable.

It is seen from Fig. 2 that the Δn of each compound varies strongly in the region of T_N . This anomalous variation of Δn can be attributed naturally to the establishment of a magnetically ordered state in the crystals. As shown by us in a preceding paper^[7], the temperature-induced change of Δn is the sum of pure magnetic birefringence and birefringence due to the temperature-induced change of the lattice constants:

$$\Delta n(T) = \Delta n_M(T) + \Delta n_{\text{lat}}(T). \quad (1)$$

We note that Δn_{lat} consists of two parts: the birefringence change Δn_{str} due to spontaneous striction, and the birefringence change Δn_{ther} due to the usual thermal expansion:

$$\Delta n_{\text{lat}} = \Delta n_{\text{str}} + \Delta n_{\text{ther}}. \quad (2)$$

To separate the purely magnetic part of the birefringence it was necessary to find $\Delta n_{\text{lat}}(T)$. The procedure for separating $\Delta n_M(T)$ was carried out for MnF_2 and CoF_2 . We shall describe it in greater detail with MnF_2 as an example.

Assume that the lattice-induced difference of refractive indices is a function of the degree of tetragonality of the crystal:

$$(n_o - n_e)_{\text{lat}} = f(a/c). \quad (3)$$

Here a and c are the constants of the tetragonal lattice. Then

$$d(n_o - n_e)_{\text{lat}} = df \left(\frac{a}{c} \right) = f' \frac{a}{c} \left(\frac{da}{a} - \frac{dc}{c} \right) = M \left(\frac{da}{a} - \frac{dc}{c} \right). \quad (4)$$

Since the lattice constants change less than by 1% in the entire temperature interval from 0 to 300°K, the quantity M can be regarded as constant for the given compound.

The validity of this treatment in the paramagnetic region is confirmed by the results of the reduction of the experimental data, shown in Fig. 12 of the paper by Jahn^[17]. It is seen from this figure, which shows the temperature dependence of the ratio $d(n_o - n_e)/(da/a - dc/c)$, that the condition $M = \text{const}$ is well satisfied for MnF_2 , CoF_2 , and FeF_2 , starting with $\sim 200-300^\circ\text{K}$ and above. For ZnF_2 , the value of M is constant in the entire measured temperature interval. We shall assume henceforth that M does not depend on whether the change of the degree of tetragonality is the result of the

usual thermal expansion or is the result of spontaneous striction.

Using the data of Gibbons^[18] for the temperature dependence of the coefficients of expansion of MnF₂, we have plotted the curve

$$\Delta n_{\text{lat}}(T) = M \left(\frac{\Delta a}{a} - \frac{\Delta c}{c} \right).$$

The coefficient M was determined from a comparison of our experimental data for $\Delta n(T)$ with the curve calculated from the data of^[18]

$$\Phi(T) = \frac{\Delta a}{a} - \frac{\Delta c}{c}$$

in the high-temperature region (see Fig. 3, and also Fig. 12 in^[17]). It is seen from Fig. 3 that starting with 200°K and below, the experimental $\Delta n(T)$ dependence does not duplicate the temperature dependence of the degree of tetragonality of the crystal lattice, $\Delta n_{\text{lat}}(T)$. The difference between these curves, which represents the temperature dependence of the magnetic birefringence $\Delta n_M(T)$, is shown in Fig. 4.

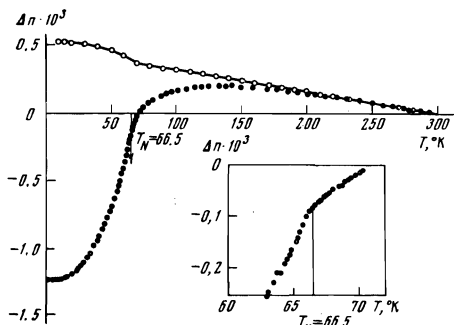


FIG. 3. Temperature dependence of the birefringence of MnF₂: ●—experimental, ○—calculated from formula (4).

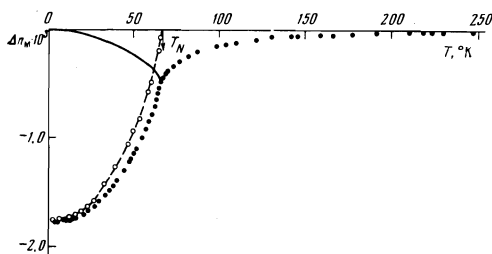


FIG. 4. Temperature dependence of the magnetic birefringence of MnF₂ (●) and of the square of the static sublattice magnetization (○) taken from the NMR experiments^[19]. The solid line corresponds to the difference between these quantities.

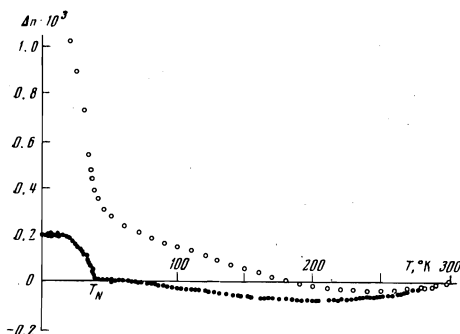


FIG. 5. Temperature dependence of the birefringence of CoF₂: ●—experimental, ○—calculated from formula (4).

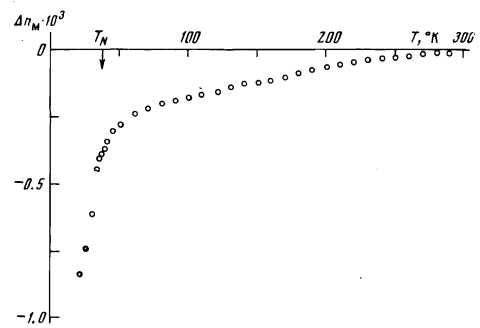


FIG. 6. Dependence of the magnetic birefringence of CoF₂ on the temperature.

The experimental data for CoF₂ (Figs. 5 and 6) were reduced by the scheme described above, using the results obtained by S. I. Novikova (Metallurgy Institute of the USSR Academy of Sciences) for the temperature dependence of the linear-expansion coefficients of CoF₂.³⁾ As seen from Fig. 5, the value of $\Delta n_{\text{lat}}(T)$ for CoF₂ is anomalously large in the ordered state (spontaneous striction). Consequently, the summary (measured) $\Delta n(T)$ has the same sign as the effect due to the spontaneous striction. This explains qualitatively the difference between the experimental $\Delta n(T)$ curves for CoF₂ and MnF₂ in Fig. 2.

For NiF₂, unfortunately, we were unable to separate the magnetic part of the birefringence, since the available experimental data of Haefner et al.^[20] do not suffice to determine the coefficient M in formula (2). It is seen from Fig. 2, however, that the behavior of Δn_M for NiF₂ should be qualitatively similar to that for MnF₂.

The experiments performed by us in the second configuration of the experiment, when the light was directed along the optical axis of the crystal, have shown that in this case there is no birefringence in any of the compounds in the entire investigated temperature interval.

The experimental results represented above enable us to draw the following conclusions:

1. Magnetic birefringence due to establishment of magnetic order is produced in MnF₂, CoF₂, and NiF₂ in the region of the Neel temperature (see also^[7]). Since MnF₂ and CoF₂ have no ferromagnetic moment in the ordered state, it follows that the resultant Δn_M can be attributed naturally to the appearance of the antiferromagnetic vector **l**. The value of Δn_M amounts to $(1 - 2) \times 10^{-3}$, which is larger by one or two orders of magnitude than in the previously investigated ferrites and antiferromagnets with weak ferromagnetism.

2. At Neel temperatures, a kink is observed on the $\Delta n(T)$ curve of MnF₂ or CoF₂. It is seen most clearly for MnF₂ in Fig. 3 (see the insert). For NiF₂, owing to the large scatter of the experimental data, it was impossible to observe the kink. The kink temperature coincide well with the positions of the maxima on the specific-heat curves $c_p(T)$ of these substances. The first to point out this circumstance were Jahn and Dachs^[8,17].

3. The results (see Figs. 3 and 5) demonstrate quite convincingly that in the case of MnF₂ and apparently also NiF₂, the main cause of the anomalous temperature dependence of birefringence is not the spontaneous striction, but the direct magnetic birefringence. In the case of CoF₂, the spontaneous striction causes a bire-

fringence change comparable with the magnetic change. The value of Δn_M is of the same sign for all three compounds, the opposite of the sign of Δn_{lat} .

4. The results show that within the limits of the accuracy of our experiments all the crystals remain optically uniaxial in the antiferromagnetic region: there is no birefringence in the case when the light is directed along a fourfold axis⁴⁾.

5. As already mentioned, the magnetic structures of the fluorides are different, namely: $1 \parallel [001]$ for MnF_2 and CoF_2 , and $1 \perp [001]$ for NiF_2 . However, a comparison of the experimental results shows that the general character of the phenomenon investigated by us is the same for all three compounds and does not depend on their magnetic structure.

6. In the case of MnF_2 , we succeeded in comparing $\Delta n_M(T)$ with the temperature dependence of the square of the sublattice magnetization \bar{l}^2 , taken from NMR data^{11,9)}, and reconciled with the $\Delta n_M(T)$ curve at liquid-helium temperatures—see Fig. 4. It is seen from Fig. 4 that Δn_M is somewhat larger than the value calculated from the NMR data.

7. Figures 4 and 6, which show the temperature dependence of the magnetic birefringence, demonstrate that Δn_M does not vanish at the Neel point, and is preserved up to temperatures $\sim (2-3)T_N$.

4. EXPERIMENTAL RESULTS AT $H \neq 0$

In the present study we investigated the effect of the magnetic field (up to ~ 50 kOe) on the birefringence of light in MnF_2 , CoF_2 , and NiF_2 . It is well known that a strong magnetic field can change the magnetic structure of the investigated compounds. In MnF_2 ^[21], a field applied at a certain angle to the fourfold axis $[001]$ leads to a deflection of the vector l away from this axis. The 50-kOe field available to us, applied at an angle $\sim 15^\circ$ to the $[001]$ axis, rotates l in MnF_2 through an angle $\sim 10^\circ$. In CoF_2 , the deflection of the vector l is negligible in such a field. However, the strong Dzyaloshinskiĭ interaction causes a deflection of the vector l from the $[001]$ axis in CoF_2 ^[22] to be produced under the influence of a magnetic field directed along the binary axis $[100]$ (or $[010]$); this gives rise to projection of the vector l along the other binary axes $l_{x,y} = l \sin \theta$, where θ is the angle between l and $[001]$. According to Ozhogin^[22], $l_{x,y} = \alpha H$ up to fields ~ 100 kOe. In NiF_2 , a magnetic field applied along one of the binary axes $[100]$ or $[010]$ does not change the magnetic structure, but orients the antiferromagnetic domains and magnetizes the sample.

The influence of the magnetic field on the birefringence was investigated by us with the following experimental configurations:

a) the magnetic field is directed along the fourfold axis $[001]$, and the light propagates along the binary axis $[010]$. In the case of MnF_2 , we also performed an experiment in which the magnetic field was applied at an angle of 15° to the $[001]$ axis.

b) A magnetic field is directed along the binary axis $[100]$ and the light propagates along the fourfold axis $[001]$.

c) Both the light and the field are directed along binary axes: $k \parallel [010]$ and $H \parallel [100]$.

In the experiments with MnF_2 and NiF_2 , we were

unable to observe any change in the birefringence with changing field in all three configurations. In the case of CoF_2 , on the other hand, it was observed that in the antiferromagnetic state the crystal becomes optically biaxial following application of a magnetic field along the twofold axis (configuration b)). This is clearly seen in Fig. 7, namely, there is practically no birefringence in the zero field, and the small effect observed at $H = 0$ can be due to inaccurate orientation of the crystal. Application of the field leads to the appearance of

$$\Delta n_H = \Delta n_{\perp H} - \Delta n_{\parallel H}.$$

The value of Δn_H is small, $\sim (1-2) \times 10^{-5}$, but it exists not only in the antiferromagnetic region, but also somewhat above T_N . In configuration c), introduction of the magnetic field leads to a decrease of the already existing Δn (see Fig. 8). The change $\delta(\Delta n)$ depends quadratically on the applied field and amounts to $\sim 3 \times 10^{-5}$ at $H \sim 50$ kOe. The influence of the field is noticeable up to temperatures $\sim 1.5T_N$.

From all these experiments, we can draw the following conclusions:

1. The fact that the birefringence of MnF_2 and NiF_2 does not change in the magnetic field indicates that the birefringence of these substances does not depend on the orientation of the vector l relative to the crystallographic axes or of the mutual arrangement of the vectors l and k . In addition, it is clear that we are observing not ordinary paramagnetic birefringence, but the so-called Cotton-Mouton effect, which is quadratic in the magnetic field:

$$\Delta n_{cm} \sim (\chi_{\perp} H)^2,$$

where χ_{\perp} is the magnetic susceptibility.

2. In CoF_2 , the susceptibility χ_{\perp} is of the same order of magnitude as in MnF_2 (see the table), so that we can

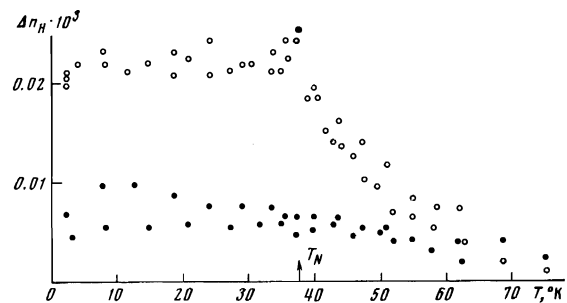


FIG. 7. Magnetic birefringence $\Delta n_H = \Delta n_{\perp H} - \Delta n_{\parallel H}$ of CoF_2 in a magnetic field at $k \parallel [001]$, $H \parallel [010]$, and $E \parallel [110]$ in the case of $H = 0$ (●) and $H = 47$ kOe (○).

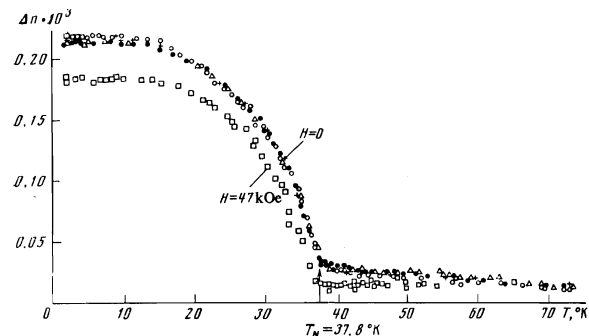


FIG. 8. Effect of magnetic field on the birefringence of light in CoF_2 in the case $k \parallel [100]$, $H \parallel [010]$, and $E \parallel [011]$.

assume that in this substance, too, the influence of the magnetic field on the birefringence is not the Cotton-Mouton effect, but is due to other causes. It appears that one can assume that the magnetic birefringence of CoF_2 is affected by the change of the magnetic structure of the crystal.

5. DIELECTRIC TENSOR

The question of the microscopic character of magnetic birefringence in antiferromagnets has been the subject of a number of theoretical papers (see, e.g., ^[23,24]). We shall attempt below to describe the observed experimental facts phenomenologically, making no assumptions whatever concerning the mechanism of the phenomenon, and using only symmetry considerations. On the basis of these considerations, the expression for the density of the internal electromagnetic energy of antiferromagnetic fluorides (space group D_{4h}^{14}), with allowance for the terms responsible for the birefringence and quadratic in the components of the antiferromagnetism vector, is given by

$$\begin{aligned} \mathcal{E} = & \mathcal{E}_0 + [\lambda_1 E_x^2 + \lambda_2 (E_x^2 + E_y^2)]^2 \\ & + \lambda_3 E_x^2 l_z^2 + \lambda_4 (E_x^2 + E_y^2) l_z^2 + \lambda_5 E_x l_z (E_x l_x + E_y l_y) \\ & + \lambda_6 E_x l_z (E_x l_x + E_y l_x) + \lambda_7 E_x E_y l_z l_y \\ & + \lambda_8 (E_x^2 - E_y^2) (l_x^2 - l_y^2) / 8\pi. \end{aligned} \quad (5)$$

As usual, the z axis is directed along the fourfold axis [001], the x and y axes coincide with the twofold axes [100] and [010], $\mathbf{l} = (\mathbf{M}_1 - \mathbf{M}_2)/2M_0$ is the antiferromagnetic vector, E_x, E_y, E_z are the components of the electric field of the incident wave, and λ_n are the magneto-optical coefficients.

In writing down (5), we started from the assumption that the birefringence in the antiferromagnets is determined primarily by the antiferromagnetic vector \mathbf{l} , since the magnitude of the magnetization vector \mathbf{m} is smaller than \mathbf{l} by 2–3 orders of magnitude.

Differentiating \mathcal{E} with respect to E_i and E_k , we obtain the components of the symmetrical tensor of the dielectric constant:

$$\begin{aligned} \epsilon_{xx} = & \epsilon_{\perp}^0 + \lambda_2 l^2 + \lambda_4 l_z^2 + \lambda_8 (l_x^2 - l_y^2), \\ \epsilon_{yy} = & \epsilon_{\perp}^0 + \lambda_2 l^2 + \lambda_4 l_z^2 - \lambda_8 (l_x^2 - l_y^2), \quad \epsilon_{zz} = \epsilon_{\parallel}^0 + \lambda_1 l^2 + \lambda_3 l_z^2, \\ \epsilon_{xy} = & \epsilon_{yx} = \lambda_7 l_x l_y, \\ \epsilon_{xz} = & \epsilon_{zx} = \lambda_5 l_z l_x + \lambda_6 l_z l_y, \quad \epsilon_{yz} = \epsilon_{zy} = \lambda_6 l_z l_y + \lambda_6 l_z l_x. \end{aligned} \quad (6)$$

Here ϵ_{\perp}^0 and ϵ_{\parallel}^0 are the principal dielectric constants of the uniaxial crystal in the paramagnetic state.

An analysis of the tensor ϵ_{ijk} (6) shows that allowance for the isotropic-exchange terms alone in the expression for the energy (5) leaves the crystal optically uniaxial following a transition to the magnetically ordered state. The magnetic birefringence produced in this case is proportional to the square of the antiferromagnetic vector:

$$\Delta n_{\mathbf{M}}^{\text{isotr}} = \frac{l^2}{2} \left(\frac{\lambda_1}{n_{\parallel}^0} - \frac{\lambda_2}{n_{\perp}^0} \right) \quad (n_{\parallel}^0 = \sqrt{\epsilon_{\parallel}^0}, \quad n_{\perp}^0 = \sqrt{\epsilon_{\perp}^0}). \quad (7)$$

The quantity $\Delta n_{\mathbf{M}}^{\text{isotr}}$ for a given substance does not depend on the direction of the vector \mathbf{l} relative to the crystallographic axes, i.e., on the magnetic structure of the compound.

It follows from the form of the tensor ϵ_{ijk} that the terms that are anisotropic with respect to the components of the antiferromagnetic vector \mathbf{l} likewise do not make the crystal biaxial if the vector \mathbf{l} is directed along the [001] axis ($l_x = l_y = 0, l_z = l$). In this case we have

$$\Delta n_{\mathbf{M}} = \frac{l^2}{2} \left[\frac{\lambda_1}{n_{\parallel}^0} - \frac{\lambda_2}{n_{\perp}^0} + \frac{\lambda_3}{n_{\parallel}^0} - \frac{\lambda_4}{n_{\perp}^0} \right]. \quad (8)$$

A comparison of the experimental data with the theoretical analysis leads to the following conclusions. The fact that the phenomenon is similar in MnF_2 and NiF_2 at $H = 0$, in spite of their different magnetic structures, suggests that in this case the predominant factor is the isotropic effect, which is due to the isotropic-exchange increment to ϵ_{ijk} . This assumption explains also why the magnitude of the birefringence is not affected, first, by the orientation of the antiferromagnetic domains by the magnetic field in NiF_2 , and, second, by the deflection of the spins away from the [001] axis in MnF_2 in a strong field. The magnetic birefringence is described in all these cases by formula (7).

In the case of CoF_2 at $H = 0$, the quantity $\Delta n_{\mathbf{M}}$ behaves in the same manner as in NiF_2 and MnF_2 , and is likewise apparently due mainly to the isotropic-exchange terms (formula (7)). However, if the crystal becomes optically biaxial below T_N , then its state can no longer be described with the aid of only the isotropic-exchange terms and the terms with l_x^2 in (5). In this case it is necessary to take into account the anisotropic terms that contain the components l_x and l_y .

Using the components of the optical indicatrix tensor $B_{ijk} = \epsilon_{ijk}^{-1}$, we calculated the change in the refractive index as a result of the transition of the crystal to the ordered state for several particular cases corresponding to the conditions of our experiments. The appearance of the l_x component changes the magnetic birefringence in the zy plane. This change is described in the formula for $\Delta n_{\mathbf{M}}$ by an additional term of an anisotropic type

$$\Delta n_{\mathbf{M}}^{\text{tot}} = n_y - n_x = \frac{l^2}{2} \left(\frac{\lambda_1}{n_{\parallel}^0} - \frac{\lambda_2}{n_{\perp}^0} \right) + \frac{l_x^2}{2} \left(\frac{\lambda_3}{n_{\parallel}^0} - \frac{\lambda_4}{n_{\perp}^0} \right) + \frac{l_x^2 \lambda_8}{2 n_{\perp}^0}. \quad (9)$$

In the derivation of (9) we took into account that the angle of rotation of the axes y and z needed to diagonalize the tensor B_{ijk} , which is given by

$$\text{tg } 2\alpha = \frac{2\lambda_8}{\epsilon_{\parallel}^0 - \epsilon_{\perp}^0} l_x l_z$$

is small, and the calculation was carried out for the original coordinate system.

At $l_x \neq 0$, birefringence is produced in a plane perpendicular to the [001] axis, and is expressed by the formula

$$\Delta n_{\mathbf{M}} = n_x - n_y = \lambda_8 l_x^2 / n_{\perp}^0. \quad (10)$$

The behavior of CoF_2 in the magnetic field agrees with formulas (9) and (10). Indeed, as already indicated above, when a field $H \parallel y$ is applied, the component l_z decreases and l_x appears. Therefore, in accord with formula (9), a change proportional to l_x^2 and consequently proportional to the square of the applied field should take place in the quantity $n_y - n_x$ (inasmuch as $l_z^2 = l^2 - l_x^2$) (Fig. 8). Formula (10) explains the birefringence observed by us in the xy [001] plane (see Fig. 7). It should be noted that the measured quantity $n_x - n_y$ is approximately one-third the change of $n_y - n_x$ resulting from application of a magnetic field. This gives grounds for assuming that the latter effect is due mainly to the influence of the term with l_z^2 in (9).

Without data on the magnetostriction of CoF_2 we were unable in the reduction of the experimental data obtained in the magnetic field, to separate the purely magnetic birefringence from the lattice birefringence due

to magnetostriction. Obviously, the increments introduced into the tensor ϵ_{ijk} by the spontaneous striction and by the magnetostriction can be represented in the form of terms that are quadratic in l_i and l_k and have the same symmetry as in (6).

6. SHORT-RANGE ORDER

As already noted, for all the investigated substances the magnetic-birefringence does not vanish at the point of the antiferromagnetic transition, and remains appreciable up to temperatures on the order of $\sim (2-3)T_N$ (Figs. 4 and 6). The presence of Δn_M above T_N can apparently be attributed to the fact that in our experiments we observe the fluctuations of the vector l (short-range order).

According to^[23,24] and Sec. 5 of the present article, the observed Δn_M is proportional in the isotropic case to the mean-squared total antiferromagnetic moment or the magnetic energy of the crystal. As a result, the mean value $\overline{\Delta(\Delta n_M)}$ due to the deviations of the vector l from its static value does not vanish. The characteristic lifetimes of the fluctuations are larger by two or three orders of magnitude than the period of the oscillations of the light wave. The fluctuations contributing to the refractive index are those in the ranges of characteristic dimensions $a \gg \lambda_{\text{light}}$ and $a \ll \lambda_{\text{light}}$. In our case at $T \sim T_N$, the condition $a \ll \lambda_{\text{light}}$ is satisfied.

A comparison of the temperature dependence $\Delta n_M(T)$ and that of the square of the static magnetization of the sublattices for MnF_2 , taken from NMR experiments^[19] (see Fig. 4), shows that even below T_N the difference $\overline{l^2} - l^2$ does not vanish, i.e., the fluctuations of the vector l are appreciable. This quantity is approximated in the case of MnF_2 by the law αT^2 in the interval from 2 to 60°K ($T_N = 66.5^\circ\text{K}$). It should be noted that this law is not a trivial consequence of spin-wave theory, since the theory is valid for $T \ll T_N$.

Short-range order in magnetically ordered systems is also observed in other experiments, such as two-magnon scattering of light, inelastic scattering of neutrons by spin waves, and measurement of the specific heat. In comparison with these experiments, ours has a number of advantages, namely, Δn itself is measured with sufficiently high accuracy and Δn_M constitutes a large fraction of the measured Δn and can be separated quite accurately if data are available on the temperature dependence of the expansion coefficient of the investigated substance.

The temperature dependence of the short-range order, according to general theoretical representations, should be represented in the region $T \gg T_N$ in the form of a series in successive powers of the reciprocal temperature:

$$A \frac{T_N}{T} + B \left(\frac{T_N}{T} \right)^2 + \dots$$

In the region T_N , the scaling-theory laws should be fulfilled^[25]. Attempts to observe these laws on our experimental curve were unsuccessful (see Fig. 9). It turned out that the accuracy of our experiments was insufficient for a comparison in the two indicated temperature regions. However, as follows from Fig. 9, the following law is satisfied in a sufficiently wide range of temperatures (70–110°K):

$$\Delta n_M \propto T^{-2.7}.$$

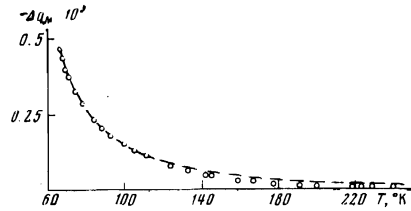


FIG. 9. Temperature dependence of the magnetic birefringence of MnF_2 at $T > T_N$. The dashed curve is a plot of $\Delta n_M \propto T^{-2.7}$.

An analysis of the tensor ϵ_{ijk} (6) shows that in the absence of a magnetic field the observed short-range order is the result of only the isotropic-exchange terms and the term l_z^2 . The anisotropic terms, which include the x and y components of the vector l , have a zero average value above T_N . When a magnetic field is applied, these anisotropic terms also make a contribution to the short-range order. This is experimentally confirmed with CoF_2 as an example.

It is interesting to note that in the case of cubic magnetically ordered crystals, where only anisotropic terms in the dielectric tensor are responsible for the magnetic birefringence, no short-range order should be observed above T_N in the absence of the magnetic field.

In conclusion, we are grateful to P. L. Kapitza for interest in the work and to I. E. Dzyalonskiĭ and D. N. Khmel'nitskiĭ for fruitful discussions.

- ¹In the case of MnF_2 and CoF_2 we operated in the region far from the absorption bands, and in NiF_2 we operated at the edge of the absorption band^[12-14].
- ²The authors are sincerely grateful to S. V. Petrov for supplying the samples
- ³The authors are sincerely grateful to S. I. Novikova for measuring the temperature dependence of the linear-expansion coefficients of CoF_2 and for kindly supplying the results of these measurements.
- ⁴In view of its magnetic symmetry, NiF_2 could have been expected to be an optically biaxial crystal (see below).

- ¹J. F. Dillon, J. Appl. Phys. **29**, 1286 (1958).
- ²R. V. Pisarev, I. G. Siniĭ, and G. A. Smolenskiĭ, ZhETF Pis. Red. **9**, 112, 294 (1969) [JETP Lett. **9**, 64, 172 (1969)].
- ³R. V. Pisarev, I. G. Siniĭ, and G. A. Smolenskiĭ, Zh. Eksp. Theor. Fiz. **57**, 737 (1969) [Sov. Phys.-JETP **30**, 404 (1970)].
- ⁴R. V. Pisarev, I. G. Siniĭ, N. N. Kolpakova, and Yu. M. Yakovlev, ibid. **60**, 2188 (1971) [33, 1175 (1971)].
- ⁵J. F. Dillon, J. P. Remeika, C. R. Staton, J. Appl. Phys. **40**, 1510 (1969); **14**, 4613 (1970).
- ⁶I. G. Siniĭ, R. V. Pisarev, P. P. Syrnikov, G. A. Smolenskiĭ, and A. I. Kapustin, Fiz. Tverd. Tela **10**, 2252 (1968) [Sov. Phys.-Solid State **10**, 1775 (1969)].
- ⁷A. S. Borovik-Romanov, N. M. Kreĭnes, and M. A. Talalaev, ZhETF Pis. Red. **13**, 80 (1971) [JETP Lett. **13**, 54 (1971)].
- ⁸I. R. Jahn, H. Dachs, Sol. St. Comm. **18**, 1617 (1971).
- ⁹R. A. Erickson, Phys. Rev. **90**, 779 (1953).
- ¹⁰R. A. Alikhanov, Zh. Eksp. Teor. Fiz. **37**, 1145 (1959) [Sov. Phys.-JETP **10**, 814 (1960)].
- ¹¹J. W. Stout, E. Catalano, J. Chem. Phys. **23**, 2013 (1955).
- ¹²V. V. Eremenko and A. I. Belyaeva, Fiz. Tverd. Tela **6**, 1967 (1964) [Sov. Phys.-Solid State **6**, 1553 (1965)].
- ¹³J. P. van der Ziel, H. J. Guggenheim, Phys. Rev. **166**, 479 (1968).

- ¹⁴M. Balkanski, P. Moch, R. G. Shulman, *J. Chem. Phys.* **40**, 1897 (1964).
- ¹⁵V. B. Tatarskiĭ, *Kristallografika i immersionnyĭ metod* (Crystal Optics and the Immersion Method), Nedra, 1965.
- ¹⁶N. N. Mikhaĭlov and S. V. Petrov, *Kristallografiya* **11**, 443 (1966) [*Sov. Phys.-Crystallogr.* **11**, 390 (1966)].
- ¹⁷I. R. Jahn, Dissertation dem Institut für Kristallographie der Universität Tübingen, FRG, 1971.
- ¹⁸D. F. Gibbons, *Phys. Rev.* **115**, 1194 (1959).
- ¹⁹V. Jaccarino, L. R. Walker, *J. Phys. Rev.* **20**, 341 (1959). K. Heller, C. B. Benedek, *Phys. Rev. Lett.* **8**, 428 (1962).
- ²⁰K. Haefner, J. W. Stout, C. S. Barrett, *J. Appl. Phys.* **37**, 449 (1966).
- ²¹S. Foner, *Magnetism*, **1**, Academic Press, 1963, p. 398.
- ²²V. I. Ozhogin, *Zh. Eksp. Teor. Fiz.* **45**, 1687 (1963) [*Sov. Phys.-JETP* **18**, 1156 (1964)].
- ²³Toru Moriya, *J. Phys. Soc. Japan* **23**, 490 (1967).
- ²⁴H. Le Gall, J. P. Jamet, *Phys. Stat. Sol.* **46**, 464 (1971).
- ²⁵M. E. Fisher, *The Nature of the Crystal State* (Russ. transl.), Mir, 1969.

Translated by J. G. Adashko
190